Design of Spectral and Panchromatic Bands for the German MOMS-02 Sensor

H. Kaufmann
Department of Photogrammetry and Remote Sensing, University of Karlsruhe, Federal Republic of Germany
D. Meißner
Messerschmitt-Bölkow-Blohm GmbH, Munich, Federal Republic of Germany
J. Bodechtel
Commission of the European Communities, JRC-Ispra, Italy
F. J. Behr
Department of Photogrammetry and Remote Sensing, University of Karlsruhe, Federal Republic of Germany

ABSTRACT: The MOMS-02 instrument is designed as a pushbroom scanning device with along-track, simultaneously acquired forward, nadir, and backward looking stereo capability and four spectral bands in the visible and ncar infrared (NIR) range. For locating and defining the width of spectral bands in the 0.4 μm to 1.1 μm range, laboratory diffuse reflectance measurements were performed. Leaves and needles of different species of deciduous and coniferous trees, as well as mineral standards and natural surfaces of rocks and soils containing $Fe^{2+/3+}$ ions, were measured and analyzed with the support of special software development. Band optimization is based on an iterative process including the spectral properties of distinct targets, solar irradiance, atmospheric transmission (LOWTRAN 6), calibration standards, and system parameters. The selected spectral bands (#1: 440 nm to 505 nm; #2: 530 nm to 575 nm; #3: 650 nm to 685 nm; and #4: 770 nm to 810 nm) were calculated for a 13.47-m by 13.47-m ground pixel size at a nominal altitude of 160 nautical miles at the equator, and a required radiometric resolution of approximately 9 bits. Priority was given to vegetation targets. The bandpass of the panchromatic nadir (IFOV: 4.49 m by 4.49 m) and off-nadir (IFOV: 13.47 m by 13.47 m) viewing stereo modules is defined at 520 nm to 760 nm.

INTRODUCTION

MOMS, ACRONYM FOR Modular Optoelectronic Multispectral/Stereo Scanner, is an Earth sensing CCD-instrument using the "pushbroom" scan principle (Meißner, 1982). The pilot system MOMS-01, a two-channel version with an instantaneous field of view (IFOV) of 20 m, was flown aboard the STS-7/11 missions mounted on the Shuttle Pallet Satellite (SPAS) platform (Bodechtel *et al.*, 1984).

MOMS-02 is a second generation system being developed by Messerschmitt-Bölkow-Blohm GmbH (MBB) under contract to the German Aerospace and Research Establishment (DFVLR), funded by the German Ministry of Research and Technology (BMFT). MOMS-02 (Figure 1) will be equipped with four spectral bands, three in the visible (VIS) and one in the near infrared (NIR) range (Kaufmann *et al.*, 1988), and an along-track stereo capability provided by one nadir and two tilted modules 21.95° fore and aft of nadir (Bodechtel *et al.*, 1988; Meißner, 1988). A digital photogrammetric system (DPS) for producing digital elevation models from this three-line array scanner was developed by Hofmann *et al.* (1982).

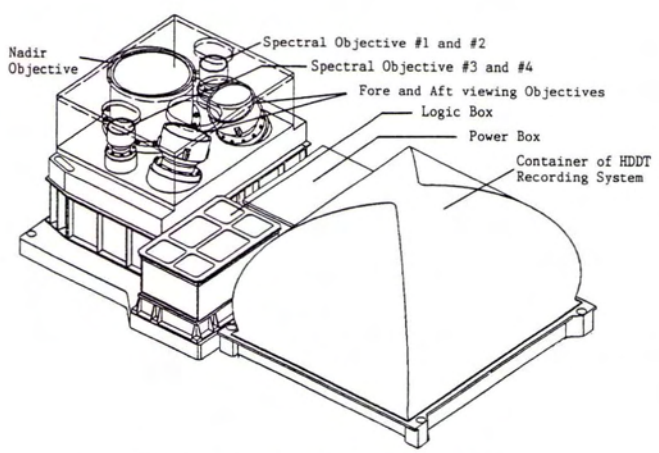

FIG. 1. MOMS-02 hardware configuration.

MOMS-02 will be flown aboard NASA's Space Shuttle during the D2 mission scheduled for 1991/92. During the mission, data will be stored on HDDT tape. Due to limitations in data transfer, MOMS will be operating in one of three different acquisition modes:

- mode 1: all spectral bands together with the panchromatic bands of the two tilted (fore and aft of nadir) modules.
- mode 2: all spectral bands together with the panchromatic band of the nadir module.
- mode 3: all panchromatic bands; nadir and tilted modules.

The swath-width of the system will be 40 km for mode 1, 60 km for mode 2, and 30 km for mode 3. This paper discusses the selection and definition of the spectral bands and the panchromatic band used for the stereo modules.

BACKGROUND

The selection of spectral bands is limited due to the complexity of parameters such as ground pixel size, detector quantum efficiency, optics transmission, atmospheric effects, signal-to-noise (S/N) ratio, data storage, etc. Within these limitations, we were able to accommodate four relatively narrow bands in the visible and NIR range. This section of the electromagnetic spectrum is characterized by the high reflectance of vegetation (mesophyll) in the NIR and the steep falloff towards the visible due to strong pigment absorptions such as chlorophyll in the 0.63-μm to 0.69-μm region and chlorophyll/carotenoid in the blue range (Tucker, 1976).

The spectral reflectance of minerals in the 0.4-μm to 1.1-μm region is mainly influenced by the wings of charge transfer bands centered in the ultraviolet and by crystal field absorptions at longer wavelengths, which are caused by transition elements. The most important transition element for terrestrial remote sensing purposes is iron in the bi- and trivalent state (Hunt and Salisbury, 1970; Hunt *et al.*, 1971).

PHOTOGRAMMETRIC ENGINEERING AND REMOTE SENSING,
Vol. 55, No. 6, June 1989, pp. 875–881.

0099-1112/89/5506–875$02.25/0

Unfortunately, we were not able to expand band definition to the short wave infrared (SWIR: 1.1 μm to to 2.5 μm) range, which would have solved the problem of enhanced recording of $Fe^{2+/3+}$ bearing materials (high reflectance in contrast to VIS/NIR-range absorptions) (Kaufmann, 1988). In addition, this would facilitate the spectral diagnostic detection of H_2O/OH^-, SO_4^{2-}, and CO_3^{2-} bearing rocks and soils derived from them (Goetz and Rowan, 1981).

The philosophy of band selection tends to place bands at regions of the spectrum where specific processes (interaction of electromagnetic energy with matter) within particular targets result in distinct spectral features. Thus, in most cases, the approach for diagnostic recording of surface features can best be met by narrow bands at sufficient S/N ratios. If adequate S/N cannot be achieved, and wider bands are necessary, or the wavelength range of interest is dominated by broad and unstable features ($Fe^{2+/3+}$ in rocks and soils), band overlap is a potential alternative to record fine details.

Therefore, we have discussed whether MOMS should be equipped with overlapping bands (Bodechtel and Kaufmann, 1985). Overlapping bands will allow the detection of slight spectral variations occurring between the band centers, although these modifications in signal can hardly be assigned to distinct features and materials. These interjacent variations in the VIS and NIR range are mainly attributable to the plurality and broad-banded character of absorptions due to ferric and ferrous ions in different crystal-field environments of rock-forming minerals and weathering products. Cross-correlations (unpubl. data) of simultaneously recorded data (corresponding TM and broader MSS bands) confirm this situation for minerals, rocks, and soils, although not for vegetation canopies, because of a relative stability of spectral characteristics in wavelength (compare Figure 2a and 2b).

Because priority of assignment for MOMS-02 is focused on the detection, differentiation, and estimation of vegetation canopies, and sufficient S/N for small-band design is attainable, the spectral band selection primarily addresses the detection of diagnostic spectral features of chlorophyll bearing targets.

METHODS

For selecting the center and width of spectral bands, *in-vivo* measurements of needles and leaves for different species of three-year-old coniferous and deciduous trees in healthy condition (Figure 2a) and progressive states of senescence or stress have been carried out. In addition, minerals, rocks, and soils of several arid test sites containing $Fe^{2+/3+}$ ions have been measured and analyzed (Figure 2b). Measurements were accomplished by use of a LAMBDA-9 Perkin Elmer laboratory spectrophotometer to obtain high resolving spectra of the relevant, signal varying pigments and ions in the wavelengths of interest.

Spectra are digitally stored in an X-tree library where they can easily be accessed and evaluated by a specially designed software package. This package has been newly developed for mathematical manipulation (e.g., ratioing, subtracting, multiplying, and normalizing) and for calculating minima/maxima and derivatives. In addition, it supports the interactive determination of band centering by minimizing/maximizing the integrals of reflectance for a given bandwidth or filter, whereby interband correlation calculations for any number and width of bands can be obtained.

To evaluate the energy available at specific wavelengths and to correct for the different attenuations due to atmospheric water vapor and molecular oxygen, the solar spectral irradiance (Figure 3; curve A) (Wolfe and Zissis, 1978) and an atmospheric model, LOWTRAN 6 (Kneizys *et al.*, 1983), were utilized to calculate the incoming radiation over a path from above the atmosphere (100 km) to 500 m above sea level (Figure 3; curve B)

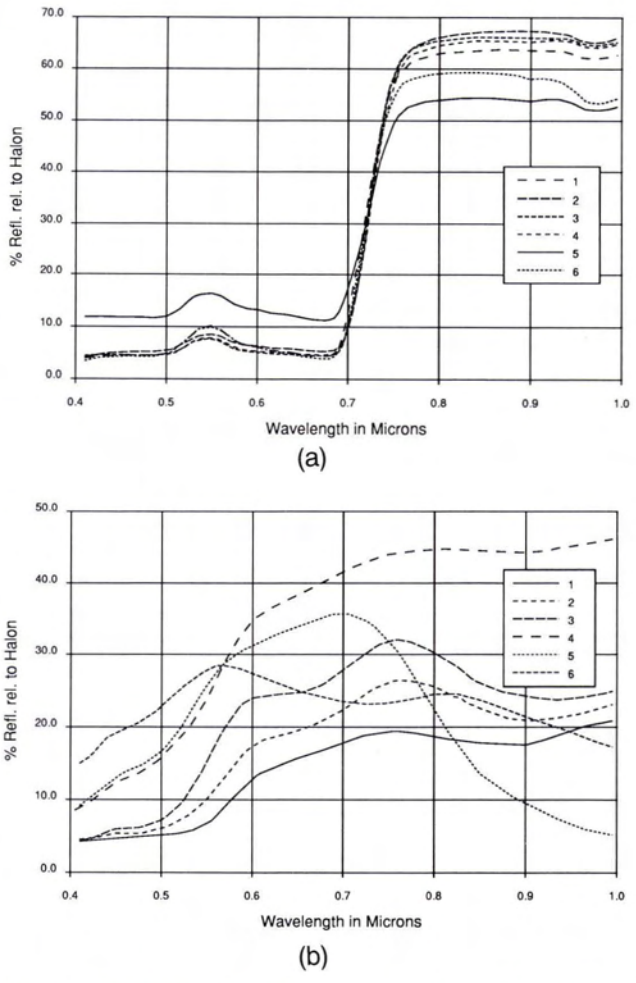

FIG. 2. (a) Selection of spectral curves of leaves and needles (*in vivo*) of different species of trees. 1: Acer pseudoplatanus (sycamore); 2: Fraxinus excelsior (ash); 3: Fagus sylvatica (beech); 4: Quercus robur (oak); 5: Abies alba (fir); 6: Pinus sylvestris (pine). (b) Selection of spectral curves of various kinds of Fe-bearing minerals and rocks. 1: bauxite; 2: hematite; 3: goethite; 4: limonite; 5: ankerite; 6: hornblende.

and upwelling back to the sensor (Figure 3; curve C) for mid-latitude summer and 23 km visibility.

Figure 4 shows mean spectra of chlorophyll and Fe-bearing targets after the spectral characteristics of solar irradiance and two atmospheric transmissions (Figure 3) were applied. These calculations are used to find the best suited atmospheric paths, to avoid the selective influence of atmospheric gases that additionally would decrease the S/N ratio and to calculate the radiometric performance (Table 1) of MOMS-02 (Meißner, 1988).

Band location is performed with regard to the spectral characteristics of vegetation, minerals, rocks, and soils, respectively, and their causal factors as pigments and $Fe^{2+/3+}$ (here with preference to vegetation), but is influenced by the bandwidth due to different slopes of absorption wings.

The distinct bandwidth for any wavelength range within the VIS/NIR range was calculated taking the following interdependent parameters into account: flight altitude, IFOV, detector sensitivity, optics, solar irradiation, atmospheric transmission, and internal calibration. Atmospheric backscattering effects increasing to shorter wavelengths have not yet been included. Baseline for the width of spectral bands were the resulting integration times for the defined ground pixel sizes, and an overall internal

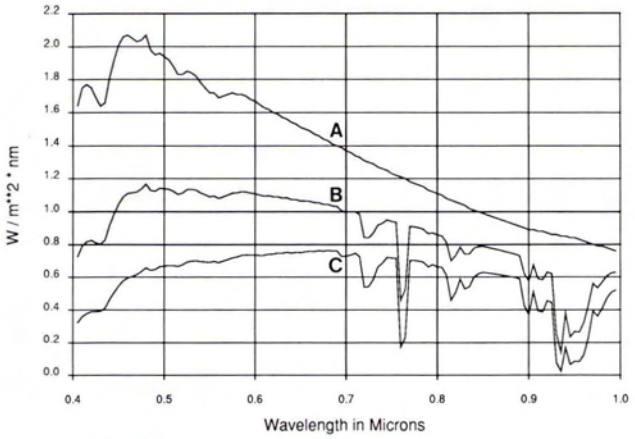

FIG. 3. Solar irradiance outside the atmosphere (A) folded once (B) and twice (C) with the spectral characteristics of a standard mid-latitude, mid-summer atmosphere for a flight altitude ≥ 100 km, a ground elevation of 500 m, and a visibility of 23 km (LOWTRAN 6 model).

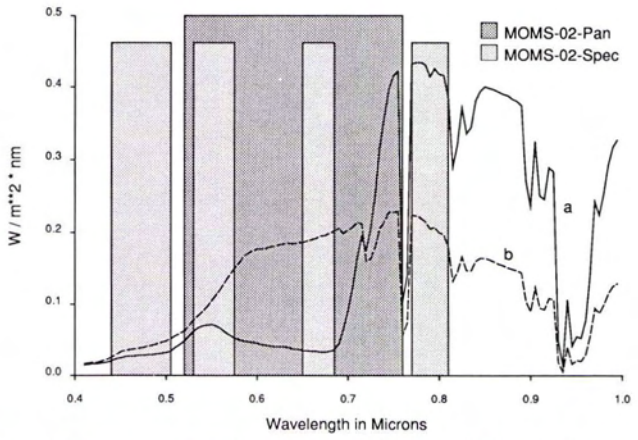

FIG. 4. Meanradiance spectra of chlorophyll (a) and Fe-bearing (b) targets with curve "C" of Figure 3 applied. Also shown are nominal bandpasses of spectral and panchromatic bands of MOMS-02.

TABLE 1. NOMINAL BANDPASSES OF MOMS-02 AND RADIOMETRIC PERFORMANCE FOR WHITE SANDS REFLECTANCE AT 70° SUN ELEVATION. NEΔρ: NOISE EQUIVALENT CHANGE OF REFLECTANCE (TARGET PLUS ATMOSPHERE PLUS INSTRUMENT).

Band Number	Nominal Band Passes (nm)	Wavelength Range	NEΔρ (%)
1	440 - 505	VIS	0.23
2	530 - 575	VIS	0.20
3	650 - 685	VIS	0.18
4	770 - 810	NIR	0.20
5,6,7	520 - 760	VIS/NIR	0.26

dynamic range of approximately 9 bits calculated for White Sands standards (Teillet, 1987) at 70° sun elevation (Meißner, 1988).

Knowing the feasible width of bands for specific wavelengths in the VIS/NIR range, the band location could be calculated on the basis of spectral characteristics (including solar irradiation and atmospheric absorptions) of the targets mentioned above (spectra in Figure 4).

This procedure is rather complex for Fe bearing targets on account of numerous unstable, mutually overlapping broad absorption wings (Figure 2b) in contrast to spectral characteristics of vegetation. Therefore, and according to the primary requirements, location of bands was calculated on the basis of healthy green vegetation, whose spectral characteristics remain almost stable with respect to the location of absorption peaks and reflectance (Figure 2a).

Our considerations for the design of the panchromatic band are similar to those made for the HRV instruments of the SPOT satellite (Begni, 1982). Band location is mainly dependent on the different spectral behavior of vegetation in contrast to rocks and soils. Bandwidth is dependent on the imaging quality of the optics, the energy available, and thus on the ground pixel size of the nadir viewing module. The energy throughput of lower resolving forward and backward tilted modules will be adapted by filters. The panchromatic bandpass of the nadir and tilted modules (fore and aft of nadir viewing) is now established at 520 nm to 760 nm. The spectral bands and the panchromatic band are also displayed in Figure 4.

DISCUSSION

MOMS-02 is designed for spectral data acquisition in the VIS and NIR range (four bands) and for along-track stereo recording using a panchromatic band for one nadir and two off-nadir looking modules. All stereo devices have equivalent bandpasses and will provide a ground pixel size of 4.49 m by 4.49 m (nadir: band 5) and 13.47 m by 13.47 m (tilted optics: bands 6 and 7). A ground pixel size of 13.47 m by 13.47 m for the spectral bands is a fair compromise to the inversely proportional spectral resolution and a noise equivalent change in reflectance (NEΔρ) of approximately 0.20 percent for all spectral bands relative to the instrument's dynamic range and noise (Table 1). In addition, the IFOV of the spectral bands and the tilted modules represents an integer multiple of that of the panchromatic nadir module, which significantly simplifies the merging of simultaneously recorded data.

SPECTRAL BANDS

Band 1: 440nm-505nm is placed within the blue absorption of vegetation that is mainly caused by chlorophyll and carotenoid concentrations (Lichtenthaler, 1987). The centering of this band is an optimization compromise controlled by atmospheric scattering at the shorter wavelength edge and the "green reflectance" (reduced pigment absorption) at longer wavelengths.

Apart from the detection of changes in pigment ratios, this band is most valuable for hydrologic applications due to shortwave transmission (penetration depth in waterbodies), and to distinguish between paved surfaces (e.g., roads, buildings) and their surroundings. Additionally, it includes the right wings of charge transfer bands (centered in the ultraviolet) that are diagnostic for Fe-bearing minerals, rocks, and soils.

Band 2: 530nm-575nm is centered at the reduced level of vegetational pigment absorption, the "green peak." It is relatively well correlated to bands 1 and 3, but can be an indicator for detecting progressive states of senescence or stress (Figure 5). It can also be useful to discriminate among rocks and soils containing ferric and ferrous iron. It has been slightly shifted from the calculated, optimized position towards longer wavelengths due to internal calibration and beam splitter requirements for the optical module that covers the first two bands.

Band 3: 650nm-685nm is directed towards the principal absorption peak for chlorophyll-*a* molecules associated with the photosynthetic light trap (Rock, 1982). It is an excellent band for *in-vivo* measurements, because there exists a strong relationship between spectral reflectance and the chlorophyll present (Tucker, 1976). The band is centered left of the calculated mean absorption maximum (675 nm) as a consequence of the

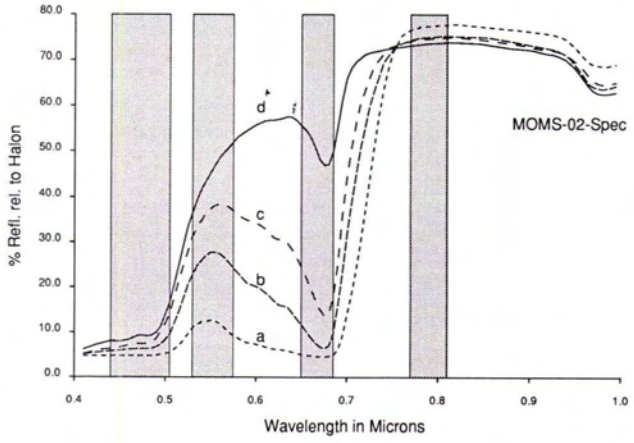

FIG. 5. Spectral curves of "prunus" with progressive states of senescence; note "blue shift" of longwave absorption wing at approximately 0.72 μm and relative fixation of absorption maxima at approximately 0.675 μm. The progression from "a" to "d" indicates increasing senescence. Also shown are nominal spectral bandpasses of MOMS-02.

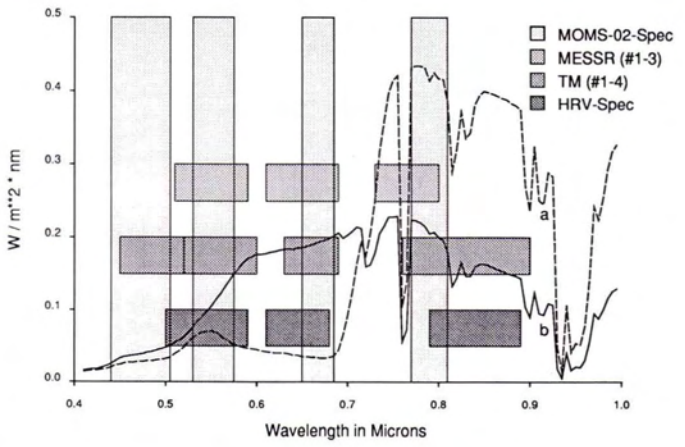

FIG. 6. Comparative illustration of nominal bandpasses of MOMS-02, SPOT—High Resolution Visible Instrument (HRV), Landsat—Thematic Mapper (TM) first four bands, MOS—Multispectral Electronic Self-scanning Radiometer (MESSR) first three bands. Bandpasses are overlain by spectra of Figure 4.

steep increase of reflectance at the so-called red edge. The blue-shift phenomenon (Collins *et al.*, 1983) will not influence the recorded signal in this band significantly (Figure 5) because it mainly affects the red edge slope, whereas the minima remain almost fixed in wavelength. In order to detect these minimal variations, the feasible bandwidths are too broad as yet. Furthermore, this band includes slight crystal field absorptions of Fe, but they are weaker than charge transfer bands and those Fe absorptions that occur at longer wavelengths.

Band 4: 770nm-810nm was essentially configured with regard to atmospheric attenuations that strongly occur at 0.76 μm (O_2,H_2O) beyond 0.89 μm (H_2O) and with less intensity at 0.82 μm (H_2O). Because of degrading sensitivity of available detectors, the region beyond 900 nm was generally restricted.

This band is placed in the high reflectance plateau of vegetation, and data derived from it can be related to biomass, state and type of cellular arrangement, density, geometry, and water content of a vegetation canopy. A strong relationship exists between spectral reflectance and the amount of green vegetation (Tucker, 1976).

In contrast to previous MOMS presentations (Kaufmann *et al.*, 1988; Bodechtel *et al.*, 1988), where band 4 was located at 830 nm to 890 nm, we decided on a shift to shorter wavelengths. This first section in the NIR window, almost unaffected by sharp features of atmospheric gases, is marked by higher energy throughput due to stronger solar irradiance. In addition, the MOMS-02 optical transmission in this region is higher and the overall bandpass of 650 nm to 810 nm (the second optic module has to cover bands 3 and 4) is less critical for correction of chromatic aberrations than a bandpass of 650 nm to 890 nm.

From a geological point of view, this newly arranged band seems to be more promising than the previous one, which only covered the shorter wavelength wings of the $Fe^{2+/3+}$ absorptions taking place at approximately 0.87 μm and at longer wavelengths.

Band 4 is now centered between the long-wavelength wings of charge transfer absorptions ($Fe^{3+} \rightarrow Fe^{2+}$/$Fe^{3+} \rightarrow O^{2-}$) in the ultraviolet, a conduction band occurring at approximately 0.55 μm and crystal field absorptions that take place at 0.64 μm, 0.87 μm, and longer wavelengths. Therefore, it is closely aligned to a relative maximum (reduced Fe absorption level) that, if used in connection with the visible range, should provide somewhat more detailed information about iron-bearing rocks and soils than can be derived from operational sensors in this region of the electromagnetic spectrum. Figure 6 shows spectral curves of Figure 4 overlain by nominal bandpasses of MOMS-02 and already existing free-flying systems.

PANCHROMATIC BAND

The major problem in defining a panchromatic band arises from the completely different spectral behavior of vegetation as compared to minerals, rocks, and soils (Figures 2a and 2b). The contrast in apparent albedo of these two categories within one single broad band, covering the VIS and NIR range, is dominated by the steep increase of reflectance of vegetation canopies at the red edge around 700 nm. To avoid confusion of similarities in apparent albedo among vegetation and rocks/soils, the location and width of the panchromatic band was investigated taking into account the spectral properties of natural targets, scattering effects, penetration depth (waterbodies), optics, and system parameters.

The shortwave edge of the panchromatic band (520 nm) is placed in order to avoid most of the noise and low-pass characteristics introduced by atmospheric scattering at shorter wavelengths, but some penetration of waterbodies is obtained. The longwave edge of the panchromatic bandpass was determined by simulating a progressive stepwise extension from 720 nm to 800 nm, using three mean reflectance plateaus (20, 40, and 50 percent) of typical vegetation canopies together with field spectra of various soils of different areas and composition (Table 2). Figure 7 shows a set of synthetized bands (linear weighted combinations) of calibrated AVIRIS data (Airborne Visible/Infrared Imaging Spectrometer) (Vane *et al.*, 1987; Vane, 1987) to elucidate the varying contrast behavior of vegetation to rocks/soils, paved surfaces, and water.

In this context, it must be stated that similarities of vegetation and rocks/soils in the albedo domain may occur, as the reflectance of the latter can vary immensely due to their mineral composition, opaque materials, and organic matter. Moreover, the assumed NIR reflectance values of vegetation may not be sufficient in terms of different textures, seasonal-phenological aspects, anisotropic reflectance, etc.

The decision for the 760-nm limit is mainly based on the transmissivity of optics and filters, simulated mean values (Table 2), and qualitative evaluation, made after linear combination of AVIRIS bands (Figure 7). User comments on panchromatic HRV-SPOT data with a bandpass of 510 nm to 730 nm have proven

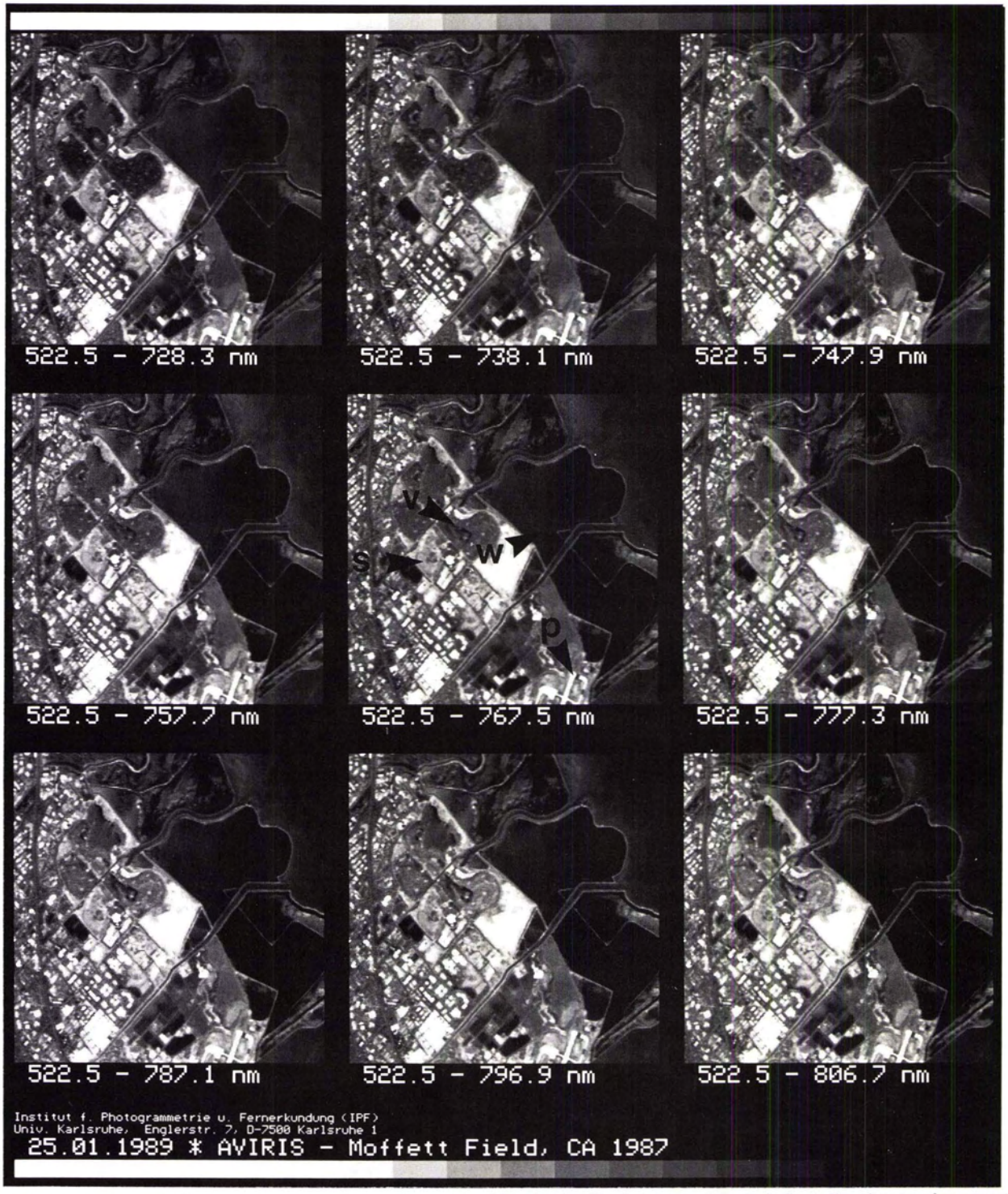

FIG. 7. Set of progressively (in steps of 9.8 nm), linearly combined bands of calibrated AVIRIS data, to indicate the change of apparent albedo for different surface categories in a broad panchromatic band. The variations in contrast of different imaged surfaces at a bandpass of 522.5 nm to 757.7 nm (bands 14 to 37) should be attributable to the defined panchromatic band of MOMS-02. Note the varying contrast ratio of vegetation (V) to soils (S), water (W), and targets consisting of asphalt or concrete (P) for different bandwidths. The increasing apparent albedo of vegetation at a continuously extended longwave edge is caused by the steep increase of reflectance at the red edge at approximately 700 nm (see also Figures 2a and 2b). The image shows a part of the Mountain View area in California (256 by 256 pixels; ground IFOV: 20 m).

that vegetation canopies are imaged insufficiently (too dark and unrefined). The extension of the panchromatic band into the NIR range will increase the apparent albedo of vegetational targets and enhance differences in intensities between distinct types and species according to greater variances in mesophyll reflectance. It slightly improves the contrast and, thus, the spatial

TABLE 2. MEAN REFLECTANCE VALUES IN % FOR DIFFERENT VEGETATION AND REPRESENTATIVE SOIL TARGETS CALCULATED FOR A STEPWISE EXTENDED PANCHROMATIC BAND* (Q = QUARTZ, FSS = FELDSPAR, CALC = CALCITE, DOL = DOLOMITE, MS = MUSCOVITE, KAOL = KAOLINITE, CHL = CHLORITE, AB = ALBITE, PX = PYROXENE, MLC = MIXED LAYER CLAY, HEM = HEMATITE, HB = HORNBLENDE, TR = TREMOLITE, CZ = CLINOZOISITE, LIM = LIMONITE).

	P_2 (nm) 520-720	P_2 (nm) 520-730	P_3 (nm) 520-740	P_4 (nm) 520-750	P_5 (nm) 520-760	P_6 (nm) 520-760	P_7 (nm) 520-780	P_8 (nm) 520-790	P_9 (nm) 520-800
Crops (NIR-reflectance ≈ 50%)	6.68	7.84	9.25	10.74	12.22	13.62	14.94	16.17	17.32
Dec. Trees (NIR-reflectance ≈ 40%)	5.47	6.43	7.58	8.80	10.01	11.16	12.24	13.25	14.19
Conifers (NIR-reflectance ≈ 20%)	2.81	3.31	3.90	4.53	5.15	5.74	6.30	6.82	7.31
Kaolinitic soil, Kaol 50%, Q 40%, Ms 10%, Saudi Arabia	61.82	61.96	62.10	62.23	62.36	62.49	62.61	62.72	62.82
Soils derived from Q-porphyry, Q 70%, Ms 10%, Fss 10%, Lim 10%, Yemen A.R.	48.25	48.67	49.08	49.47	49.84	50.17	50.46	50.73	50.97
Carbonatic soil, Dol 60%, Calc 30%, Fss 10%, Yemen A.R.	28.11	28.42	28.71	28.99	29.27	29.53	29.78	30.04	30.26
Sandy Fe-bearing soil, Calc 40%, Mlc 30%, Q 20%, Kaol 5%, Hem 5%, Jordan	22.47	22.87	23.24	23.59	23.91	24.21	24.49	24.74	24.97
Soils derived from metamorphic series, Tr 40%, Chl 30%, Cz 20%, Fss 10%, Saudi Arabia	18.83	18.78	18.73	18.68	18.64	18.59	18.55	18.51	18.47
Soils derived from eruptive material, Ab 70%, Px 20%, Q 5%, Hb 5%, Morocco	9.57	9.70	9.83	9.95	10.06	10.16	10.24	10.27	10.19

*Note the increasing similarities in apparent albedo among soils derived from eruptive and metamorphic rocks and conifers for an increasing extension of the longwave edge (P_1 to P_9).

resolution (quantitative three-dimensional application!) because of less scattered radiation and improved modulation transfer, without creating strong shadows or similar albedos for adjacent soil or rock surfaces.

A shift of the right edge of the band to shorter wavelengths diminishes recorded vegetational reflectance enormously, which deleteriously affects interpretation of products, e.g., merged images of high resolving albedo with lower resolved spectral information. Extending the right edge of the band to longer wavelengths would result in an increase in the similarities in apparent albedo of vegetation and rocks/soils, and the decrease in transmissivity of the optics would have an adverse influence on imaging quality and, thus, measuring accuracy.

SUMMARY

In the framework of the D2-mission, scheduled for 1991/92, further development of the MOMS system for multispectral/stereoscopic data acquisition was approved and set up. We had the possibility to accomodate four spectral bands in the visible and NIR range and to design a panchromatic bandpass for one nadir and two off-nadir viewing modules used for along-track stereo scanning. The definition of the width and location of spectral bands is based on spectral signatures of relevant objects, in our case on vegetation and Fe-bearing rocks and soils. Laboratory spectra were "corrected" for solar irradiation and attenuations introduced by atmospheric gases. Having defined the feasible bandwidths at sufficient S/N under consideration of radiative transfer, IFOV, and system parameters, location of bands can be established by minimizing/maximizing the integrals of a given reflectance at relevant wavelengths sections. The definition of the panchromatic band is primarily dependent on the differences of apparent albedo of soils versus vegetation due to the steep increase of reflectance of the latter at the so-called red edge.

The experimental MOMS-02 sensor is a second-generation instrument focused on detection, differentiation, and estimation of vegetation canopies and designed to provide DTMs of high quality from along-track stereoscopic data. Studies on combined elaboration and interpretation of multispectral/stereoscopic data, bidirectional reflectance, and developments of concepts for data processing and evaluation will be accomplished in advance.

ACKNOWLEDGMENTS

This research was carried out in the framework of the project "Untersuchungen zur Optimierung zukünftiger MOMS Sensoren," funded by the German Ministry of Research and Technology (BMFT). The authors wish to thank Dieter Bannert (BGR Hannover) for providing spectrophotometer access for spectral measurements and Karl Jung and Werner Weisbrich for additional programming. Special thanks to Gregg Vane for providing calibrated AVIRIS data and the permission for publication, and to the reviewers for critical comments.

REFERENCES

Begni, G., 1982. Selection of the optimum spectral bands for the SPOT satellite. *Photogrammetric Engineering and Remote Sensing*, 48–10, pp. 1613–1620.

Bodechtel, J., D. Meißner, P. Seige, R. Haydn, and H. Winkenbach, 1984. MOMS-01 on STS-7 and STS-11—missions and results. *Proc. of IGARSS Symp.*, Strasbourg, France, ESA SP-215, ESTEC, pp. 29–32.

Bodechtel, J., and H. Kaufmann, 1985. Future MOMS developments – discussion of improvements and possibilities to be expected for geologic applications. *Proc of EARSeL/ESA-Symp., European Remote Sensing Opportunities*, Strasbourg, France, ESA SP-233, ESTEC, pp. 93–96.

Bodechtel, J., F. Ackermann, D. Meißner, H. Kaufmann, P. Seige, H. Winkenbach, and J. Zilger, 1988. Development of MOMS to a future multiband and stereoscopic sensor. *Proc. of the 4th Int. Symp.*

on Spectral Signatures of Objects in Rem. Sens., Aussois, France, ESA SP-287, ESTEC, 479–482.

Collins, W., S. H. Chang, F. Raines, F. Canney, and R. P. Ashley, 1983. Airborne biogeophysical mapping of hidden mineral deposites. *Economic Geology*, 78, pp. 737–749.

Goetz, F. H. A., and L. C. Rowan, 1981. Geologic remote sensing. *Science*, 211, pp. 781–791.

Hofmann, O., P. Nave, and H. Ebner, 1982. DPS—A digital photogrammetric system for producing digital elevation models (DEM) and orthophotos by means of linear array scanner imagery. *Proc. of the Symp. on Mathematical Models, Accuracy Aspects and Quality Control*, Helsinki, Finland, ISPRS-III, 216–227.

Hunt, G. R., and J. W. Salisbury, 1970. Visible and near-infrared spectra of minerals and rocks: I. Silicate minerals. *Modern Geology*, 1, pp. 238–300.

Hunt, G. R., J. W. Salisbury, and C. J. Lenhoff, 1971. Visible and near-infrared spectra of minerals and rocks—III: Oxides and hydroxides. *Modern Geology*, 2, pp. 195–205.

Kaufmann, H., 1988. Mineral exploration along the Aqaba-Levant structure by use of TM-data; Concepts, processing and results. *International Journal of Remote Sensing*, 9, 10/11, pp. 1639–1658.

Kaufmann, H., D. Meißner, J. Bodechtel, F. J. Behr, R. Geerken, and K. Jung, 1988. Design of spectral bands for the German MOMS-02 sensor. *Proc. of the 4th Int. Symp. on Spectral Signatures of Objects in Rem. Sens.*, Aussois, France, ESA SP-287, ESTEC, pp. 425–430.

Kaufmann, H., F-J. Behr, R. Geerken, H. Jacobs, K. Jung, T. Vögtle, and W. Weisbrich, 1988. Untersuchungen zur Optimierung zukünftiger MOMS-Sensoren. *BMFT-Endbericht zum Vorhaben* 01QS86206, 53 p.

Kneizys, F. X., E. P. Shettle, W. O. Gallery, J. H. Chetwynd, L. W. Abreu, J. E. A. Selby, S. A. Clough, and R. W. Fenn, 1983. *Atmospheric Transmittance/Radiance: Computer Code LOWTRAN 6*. Air Force Geophysics Laboratory, AFGL-TR-83-0187.

Lichtenthaler, H. K., 1987. Chlorophylls and carotenoids: Pigments of photosynthetic biomembranes. *Methods in Enzymology*, 148 (34), pp. 350–382.

Meißner, D., 1982. Modular optoelectronic multispectral scanner (MOMS) development. *20th Goddard Memorial Symp. and 4th Joint AAS/DGLR Symp.*, AAS-82, 131, NASA-GSFC.

———, 1988. *Preliminary design review of MOMS-02 for D2 mission*. Doc. No: MOMS-02.RP.0010, DFVLR/MBB, 104 p.

Rock, B. N., 1982. Spatial and spectral resolution necessary for remotely sensed vegetation studies. *The Multispectral Imaging Science Working Group: Final Report*, III, NASA C.P.-2260, pp. 82–86.

Teillet, P. M., 1987. Reflectance measurements at White Sands/New Mexico using mobile spectroscopy laboratory. *Proc. of 11th Canadian Symp. on Rem. Sens.*, (in press).

Tucker, C. J., 1976. Sensor design for monitoring vegetation canopies. *Photogrammetric Engineering and Remote Sensing*, 42–11, pp. 1399–1410.

Vane, G., 1987. First results from the Airborne Visible/Infrared Imaging Spectrometer (AVIRIS). *Proc. of SPIE on Imaging Spectroscopy II*, 834, San Diego, California, pp. 166–174.

Vane, G., T. G. Chrien, E. A. Miller, and J. H. Reimer, 1987. Spectral and radiometric calibration of the Airborne Visible/Infrared Imaging Spectrometer (AVIRIS). *Proc. of SPIE on Imaging Spectroscopy II*, 834, San Diego, California, pp. 91–105.

Wolfe, W. L., and G. J. Zissis (ed.), 1978. *The infrared handbook*. The Infrared Information and Analysis (IRIA) Center, ERIM, Washington, D.C.

(Received 16 August 1988; revised and accepted 3 March 1989)

Call for Papers

Analytical Cartography

1 October 1989 Deadline for January 1991 Special Issue of the *American Cartographer*

The editors of the *American Cartographer* are soliciting papers for a special issue on analytical cartography to be published in January 1991. Potential topics include:

- Conceptual structure of analytical cartography
- Theory of spatial operators in regular/irregular cellular systems
- Spatial filtering in cartography
- Spatial data structures
- Relational data structures in a cartographic setting
- Object-oriented data structures
- Mathematical definition of cartographic objects
- Spatial database systems
- Numerical terrain analysis/representation
- Cartographic query languages
- Use of artificial intelligence in cartography
- Concepts of vehicle navigation systems
- Use of fractals in cartography
- Concepts of numerical map generalization
- New work in map projections

Prospectus due date is **1 October 1989**; manuscript submission is **1 February 1990**; notification of review is **1 May 1990**; revision of manuscript is **1 September 1990**. All manuscripts submitted will be peer reviewed. For style requirements refer to the July, 1989 issue of *American Cartographer*.

Please contact the guest editor if you are interested in a topic not listed here and send a one-page prospectus if you are interested in writing an article:

Prof. Harold Moellering
Dept. of Geography 103 BK
Ohio State University
Columbus, OH 43210
614-292-2608
Bitnet: Ts0215@OHSTVMA